PNAS
www.pnas.org

Supplementary Information for

Raf Kinase Inhibitory Protein (RKIP) Regulates the cAMP-dependent Protein Kinase Signaling Pathway Through a Positive Feedback loop

Jiyoung Lee1^#, Cristina Olivieri2#, Colin Ong1†, Larry R. Masterson2‡, Suzana Gomes1, Bok-Soon Lee4, Florian Schaeffer5, Kristina Lorenz5,6, Gianluigi Veglia2,3*, and Marsha Rich Rosner1*

Corresponding authors:

Marsha Rosner, Ben May Department for Cancer Research, University of Chicago, 959 East 57th Street, Chicago, IL 60614. Phone: (773) 702-0380; ORCID: 0000-0001-6586-8335. Email: mrosner@uchicago.edu

Gianluigi Veglia Department of Biochemistry, Molecular Biology & Biophysics, University of Minnesota 321 Church Street SE, Minneapolis, MN 55455. Phone: (612) 625 0758, ORCID: 0000-0002-2795-6964. Email: vegli001@umn.edu

This PDF file includes:

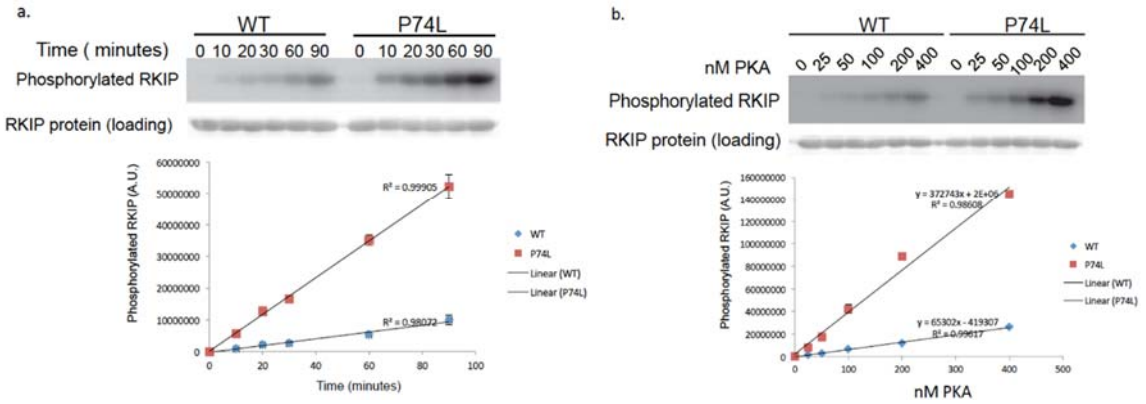

Fig. S1. PKA phosphorylates WT and P74L RKIP in a time- and dose-dependent manner. (a) PKA phosphorylates RKIP substrates in a time-dependent manner. Phosphorylation of RKIPWT and P74L mutant was assessed by in vitro kinase assay as a function of time for up to 90 minutes. The concentration of RKIP tested for each time point was 12 μM. The reaction was visualized by phosphorimaginig. Quantification of the reaction products was performed using ImageQuant 5.2 software and expressed as arbitrary units. Loading was monitored by probing the membranes with anti-RKIP antibody. (b) PKA phosphorylates RKIP substrates in a concentration-dependent manner. Phosphorylation of $RKIP^{WT}$ and P74L was determined with increasing concentrations of PKA and was quantitated as described. The error bars show the range of values measured from the two independent experiments.

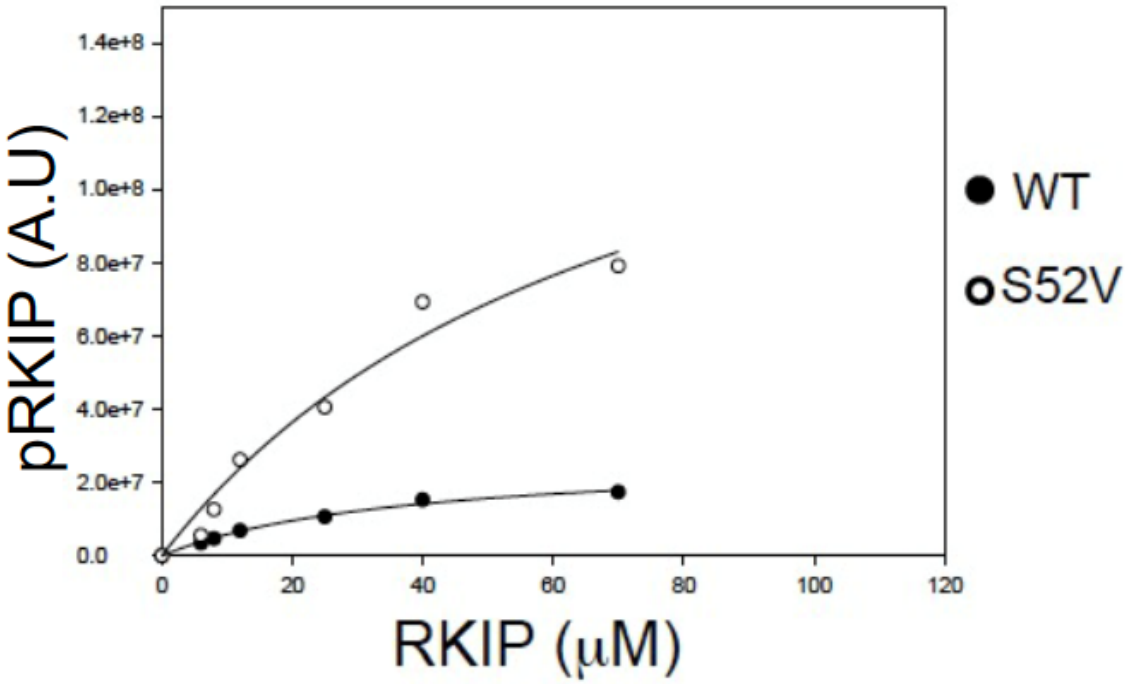

Fig. S2. Plot of the rates of phosphorylation of wt or S52V RKIP versus RKIP concentration. RKIP was assayed for PKA phosphorylation at different concentrations, and the rate of RKIP phosphorylation was determined. The phosphorylation levels were quantified using ImageQuant 5.2 software and were normalized to RKIP protein levels quantified by immunoblotting with anti-RKIP antibody and analyzed using Licor ImageStudio. To compare the phosphorylation between the various mutants, samples were normalized to the value for the WT RKIP protein. The fold induction shown in the bar graphs is an average of three independent experiments, and the error bars indicate the standard error of the mean (S.E.M).

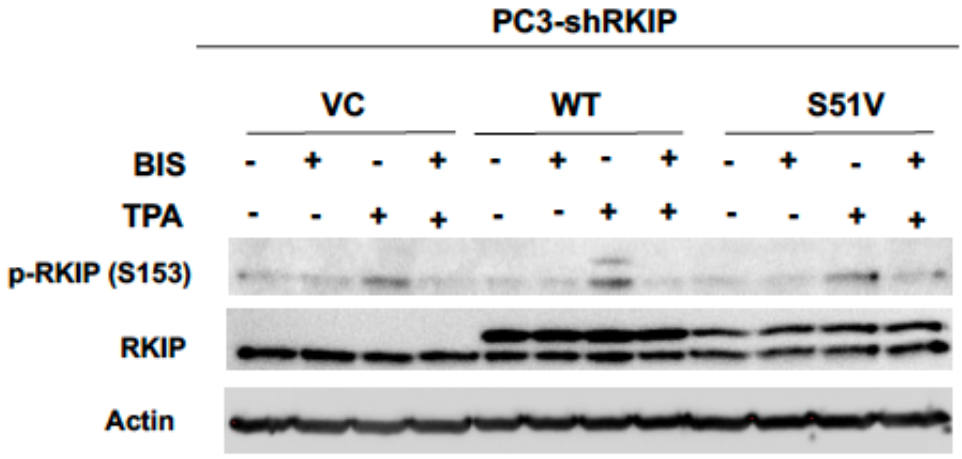

Fig. S3. Phosphorylation at Serine 153 of WT RKIP and mutant S51V RKIP in prostate tumor cells by a selective PKC inhibitor. PC-3 cells expressing RKIP ^{WT} or RKIP ^{S51V} were treated with 5 μM of Bisindolylmaleimide (BIS) for 90 minutes followed by TPA treatment for 30 minutes. The phosphorylation levels of RKIP were visualized by immunoblotting with anti-phospho-S153-RKIP (p-RKIP) antibody.

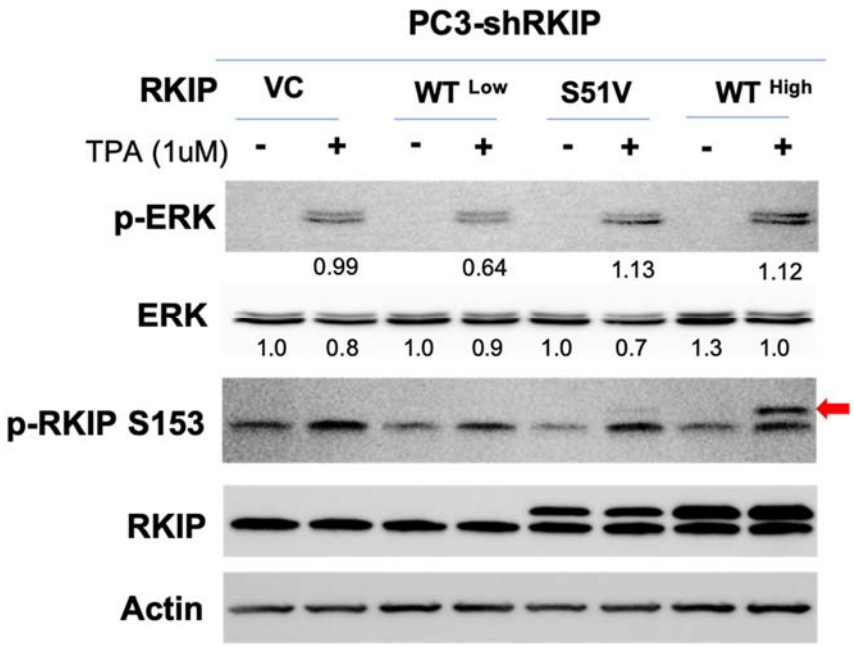

Fig. S4. ERK activation is not affected by RKIP when TPA activates PKC in prostate tumor cells. PC-3 cells expressing RKIP ^{WT} or RKIP ^{S51V} were treated with 1 μM TPA for 30 minutes after 20 hours of serum starvation. The phosphorylation levels of ERK were visualized by immunoblotting with anti-phospho-ERK (p-ERK) antibody and quantified by band density using ImageJ software.

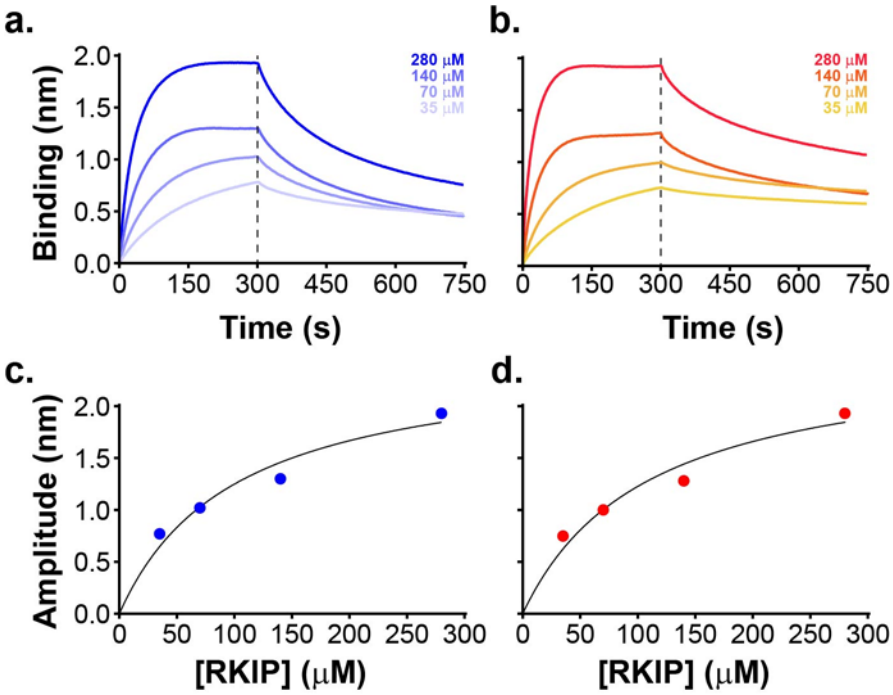

Fig. S5. Kinetic analysis by bio-layer interferometry of the binding of RKIP to apo and ATPγN-saturated PKA-C. (**a and b**) Sensograms of the His-tagged PKA-C apo (**a**) and ATPγN-bound (**b**) form. The enzyme was immobilized to an NTA biosensor and interactions were evaluated at different $RKIP^{WT}$ concentrations (35, 70, 140 and 280 μM) as reported. (**c and d**) Binding amplitude plots for the interactions of RKIP with apo and ATPγN-bound PKA-C. The data points were fitted using a non-linear regression with 1:1 stoichiometry using GraphPad9®. The calculated binding constants and cooperativity coefficients are reported in **Table 2**. The points in the graph are reported as the average of three independent experiments.

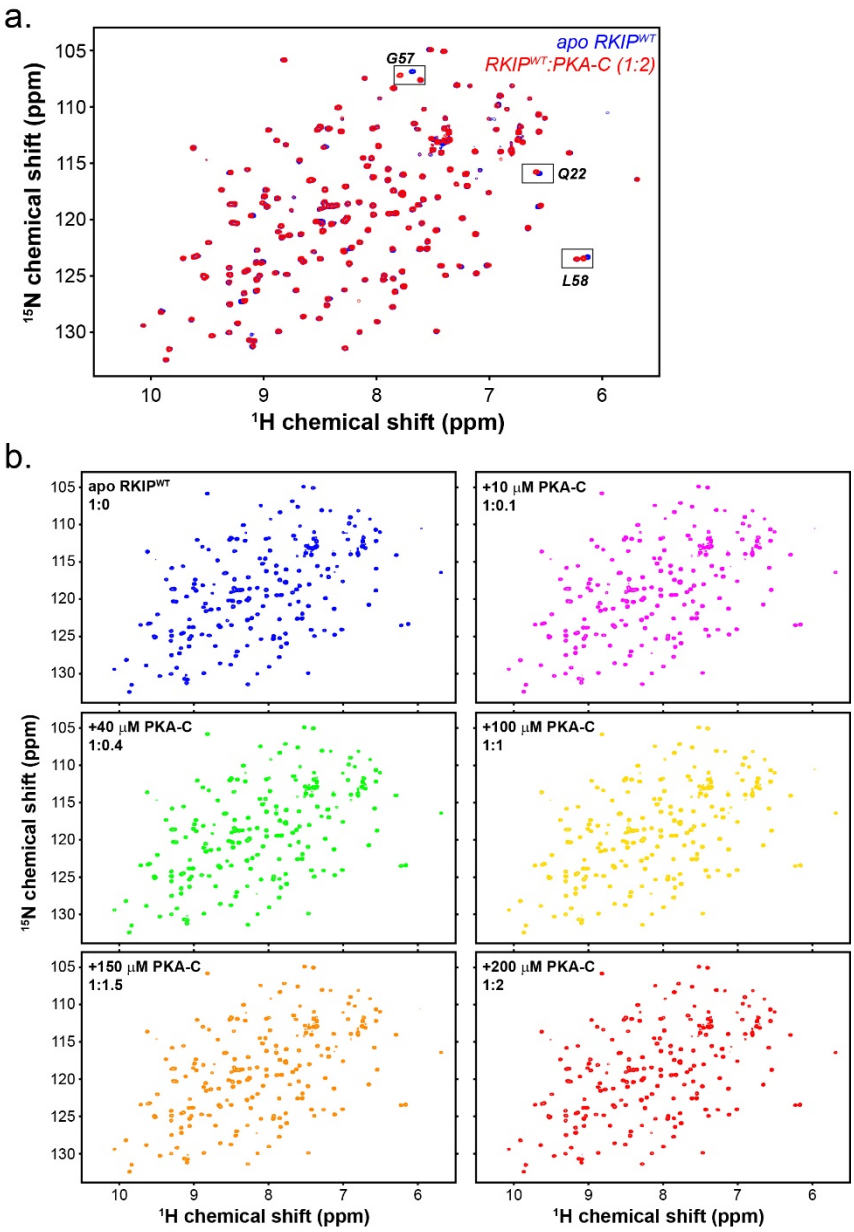

Fig. S6. NMR titration of unlabeled PKA-C/ATPγN to ^{15}N RKIP^{WT}. (**a**) [^{1}H,^{15}N]-Heteronuclear single quantum correlation (HSQC) spectra of free RKIP^{WT} and in complex with PKA-C/ATPγN (1:2 molar ratio). The two spectra were used to calculate the chemical shift perturbation (CSP) profile reported in figure 4c. The resonances in the boxes correspond to the residues in **figure 4a**. (**b**) Series of [^{1}H,^{15}N]-HSQC spectra obtained by titrating increasing amount of unlabeled PKA-C/ATPγN to ^{15}N RKIP^{WT} (1:0, 1:0.1, 1:0.4, 1:1, 1:1.5, 1.2, RKIP:PKA-C molar ratio).

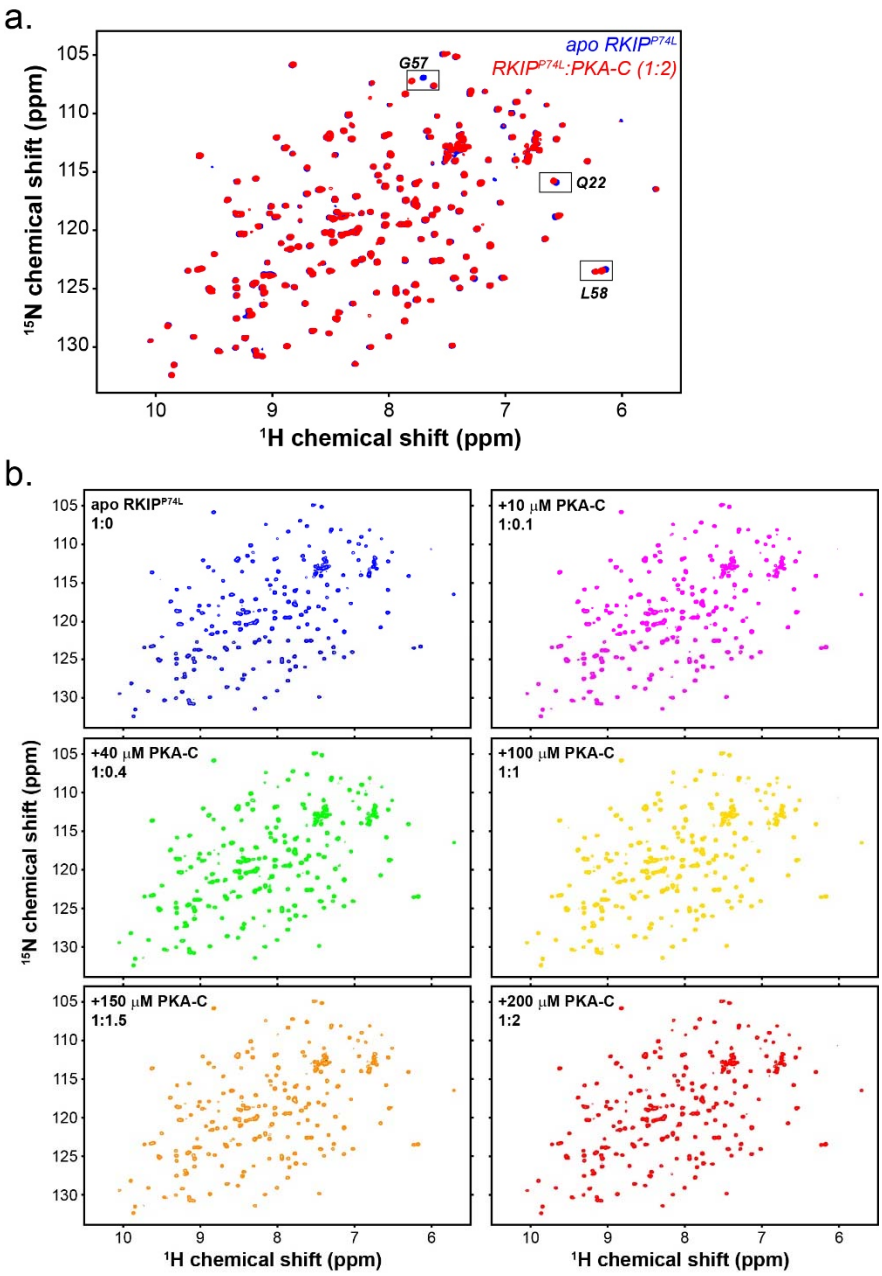

Fig. S7. NMR titration of unlabeled PKA-C/ATPγN to ^{15}N RKIP^{P74L}. (**a**) Overlay of [^{1}H,^{15}N]-HSQC spectra of free ^{15}N P74L RKIP mutant and in complex with unlabeled PKA-C/ATPγN (1:2 molar ratio). The resonances in the small squares correspond to the residues in **figure 4b**. (**b**) Series of [^{1}H,^{15}N]-HSQC spectra obtained by titrating increasing amount of unlabeled PKA-C/ATPγN to ^{15}N RKIP^{P74L} (1:0, 1:0.1, 1:0.4, 1:1, 1:1.5, 1.2, RKIP:PKA-C molar ratio).

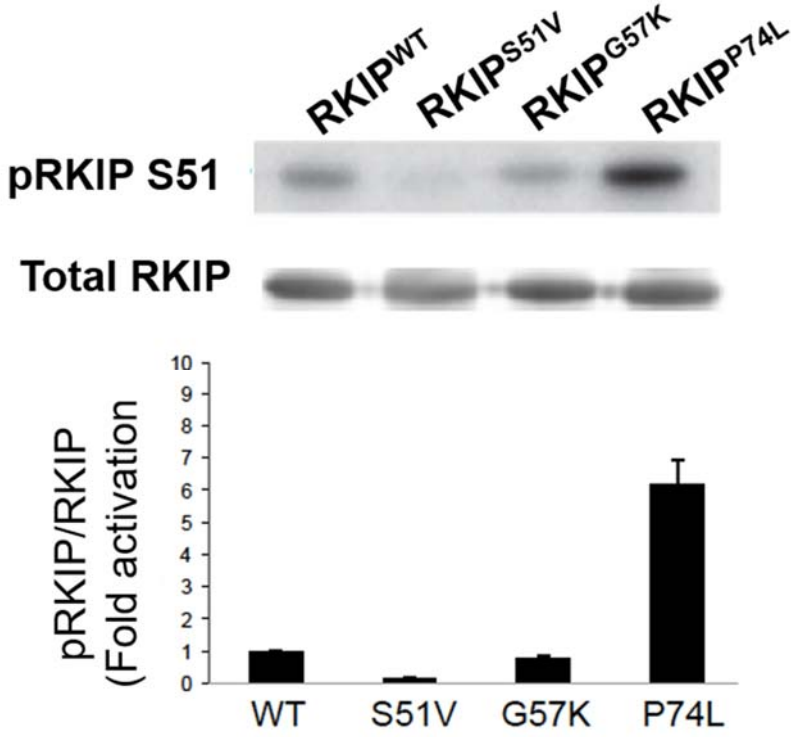

Fig. S8. Mutation of RKIP residues perturbed by PKA binding alters phosphorylation of RKIP by PKA. Phosphorylation of $RKIP^{WT}$ and mutant RKIP (S51V, G57K, and P74L) at S51. *In vitro* kinase assays were performed and RKIP phosphorylation levels were quantified using ImageQuant 5.2 software and these values were normalized to RKIP protein levels quantified by immunoblotting with anti-RKIP antibody and analyzed using Licor ImageStudio. To compare the phosphorylation between the various mutants, samples were normalized to the value for the $RKIP^{WT}$ protein. The fold induction shown in the bar graphs is an average of three independent experiments, and the error bars indicate the standard error of the mean (S.E.M).

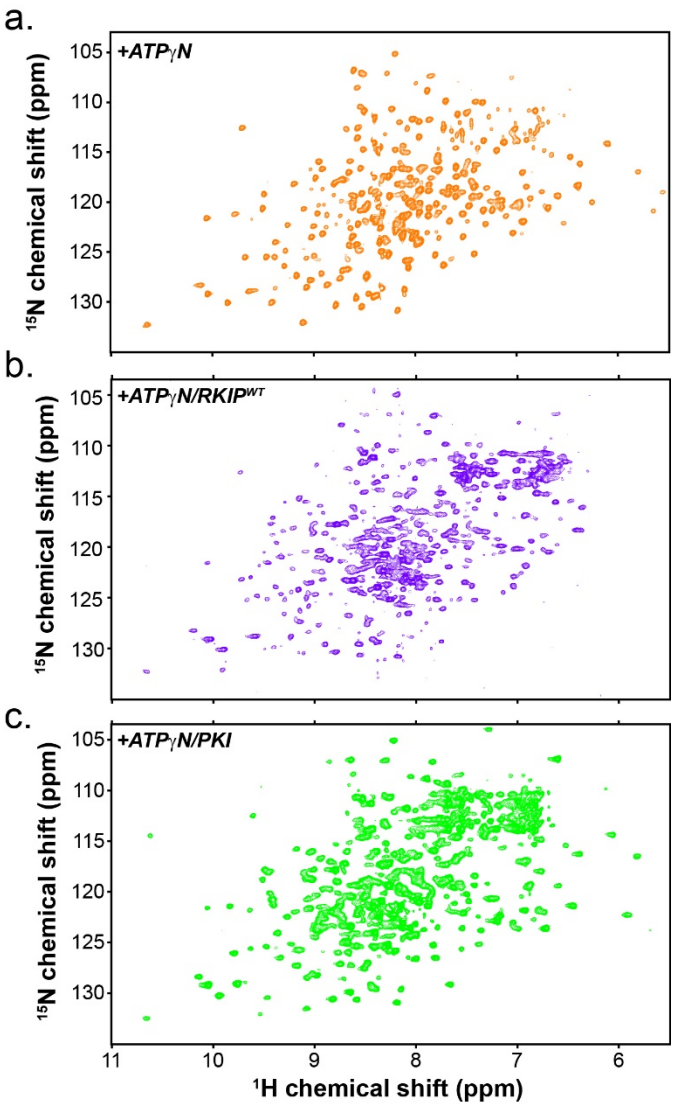

Fig. S9. ^{15}N-TROSY spectra of PKA-C in the binary complex with ATP-analog and in the ternary complex with substrate or pseudosubstrate. (**a**) [1H-^{15}N]-TROSY-HSQC spectrum of ^{15}N PKA-C saturated with ATPγN. (**b**) [1H-^{15}N]-TROSY-HSQC spectrum of PKA-C in complex with ATPγN and unlabeled-RKIP^{WT} (1:1.2 molar ratio). (**c**) [1H-^{15}N]-TROSY-HSQC spectrum of PKA-C/ATPγN/PKI complex (1:1.2 molar ratio). The chemical shift changes between the spectra in panel a and b and panel a and c are reported in the CSP profile in figure 6a in black and in blue, respectively. The spectra in panel a and b are adapted from Walker *et al.* (1).

Table S1. List of the backbone amide resonances of PKA-C/ATPγN complex that disappear upon the addition of $RKIP^{WT}$.

Residues that disappear in the ternary complex	Residue that are stabilized by in the ternary complex
E31	F43
A34	K47
L49	R133
K63	I174
K72	I303
Y146	Y330
D161	
R165	
D166	
A188	
W196	
L198	
A206	
I209	
I210	
I244	
Q245	
I246	
I250	
F314	
K343	
G344	
E346	

SI References

Sample References:

1. C. Walker *et al.*, Cushing's syndrome driver mutation disrupts protein kinase A allosteric network, altering both regulation and substrate specificity. *Sci Adv* **5**, eaaw9298 (2019).